ISBN: 978-3-95450-227-1 ISSN: 2673-5490 doi:10.18429/JACoW-IPAC2022-THPOTK007

# MAGNET SYSTEMS FOR KOREA 4GSR LIGHT SOURCE*

D. E. Kim†, Y. G. Jung, H. S. Suh, H. G. Lee, G. Hahn, T. G. Ha, J. Lee, S. S. Shin,
Pohang Accelerator Laboratory, POSTECH, Pohang, KyungBuk, Republic of Korea

*Abstract*

A 4th generation storage ring based light source is being developed in Korea since 2021. It features < 100 pm rad emittance, about 800 m circumference, 4 GeV e-beam energy, full energy booster injection, and more than 40 beamlines which includes more than 24 insertion device (ID) beamlines. This machine requires about 1000 magnets including dipole, longitudinal gradient dipole, transverse gradient dipole, sextupoles, and correctors. The apertures are small and the lattice space requirements are very tight. In this report, a preliminary design of the each magnet is presented with detailed plan for the future.

## INTRODUCTION

Third generation storage ring based light sources have been used as a bright light source for many years. Recently multi-bend achromat (MBA) lattice presents a further decrease in the electron beam emittances and becoming a new standard for next generation light source like MAX-IV in Swden, ESRF-EBS in France, SIRIUS in Brazil. Many other laboratories are also preparing their own version of 4th generation light sources. In this context, Korea is trying to build a 4th generation light source (Korea-4GSR) based on modified hybrid multi-bend achromat lattice (MHMBA). The Korea fourth-generation storage ring (Korea-4GSR) adopt H7BA considering better nonlinear beam dynamics compared to the conventional 7BA and lower emittance compared to MH6BA [1].

We reiterate simple representation of magnet higher order components to evaluate the calculated magnetic field. Using Habach convention [2], for 2-dimensional magnet which has a longer magnetic length compared to the gap, we can write the complex potential $F = A + iV$ and expand it as a series of $z = x + iy$ as

$$F = A(x,y) + iV(x,y) = \sum_{n=1}^{\infty} c_n \frac{z^n}{r_0^n} = \sum_{n=1}^{\infty} c_n \frac{(x+iy)^n}{r_0^n}. \quad (1)$$

Here, A is a vector potential, and V is a scalar potential for the magnetic field satisfying Cauchy-Riemann conditions. Using the complex potential, transverse magnetic field can be expressed as

$$B_x - iB_y = i\frac{dF}{dz} = \sum_{n=1}^{\infty} \frac{inc_n}{r_0}\left(\frac{z}{r_0}\right)^{n-1} = \sum_{n=1}^{\infty} \frac{inc_n}{r_0}\left(\frac{x+iy}{r_0}\right)^{n-1} \quad (2)$$

We can write $c_n = a_n + ib_n$, where $b_n$ is the skew components of the magnet, while $a_n$ is a normal component of the magnet.

In terms of a polar coordinate $z = x + iy = re^{i\theta}$, we can express the $B_y(\theta)$ along the radius $r$ as

$$B_y(r,\theta) = \sum_{n=1}^{\infty} \frac{-na_n}{r_0}\left(\frac{r}{r_0}\right)^{n-1} \cos((n-1)\theta) \quad (3)$$

Please note that in this indexing scheme, $n = 1$ is dipole, $n = 2$ is quadrupole, $n = 3$ is a sextupole components. In analyzing a magnet, we calculate the $B_y$ along a circle at a slice (usually 1 mm thick) and decompose it according to Eq. (3) to analyze the longitudinal dependence of a multipole content.

## MAGNET SYSTEM

### *Longitudinal Gradient Magnet*

In most types of 4GSR based light sources, longitudinal gradient magnet is routinely used to achieve low bending field in high dispersion area. APS-U [3] tried a continuous gap longitudinal gradient magnet, and also stepped field and finally opted for stepped magnetic field distribution. There are two options in achieving the design stepped field. One option can be a permanent magnet (PM) based distribution like ESRF-EBS [4], and other option can be electromagnetic magnet excitation. PM excitation has an advantage of compact magnet size, and nearly zero operating energy costs. However, there is a possibility of long term degradation (although small) due to the radiation damage, higher manufacturing costs, and lack of tunability. ESRF-EBS is adopting $Sm_2Co_{17}$ for their longitudinal gradient magnet which shows minimal radiation damage. APS-U design is based on the electromagnetic excitation. It has advantages in simpler construction, lower construction costs, and tunability. We opted for electromagnet excitation for our baseline

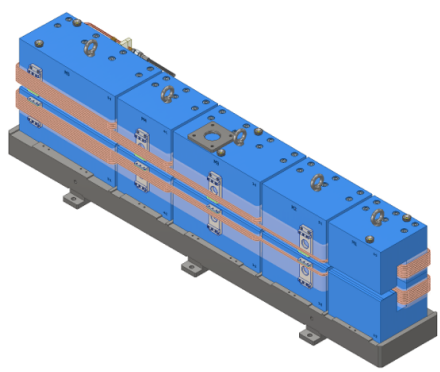

Figure 1: L3D design of LGBM1 magnet.

design considering the advantages. The 2D optimization is calculated using simple trapezoidal shims, and integrated uniformity for each segment is calculated to estimate the

* Work supported by MOST of Korea
† dekim@postech.ac.kr

ISBN: 978-3-95450-227-1 ISSN: 2673-5490 doi:10.18429/JACoW-IPAC2022-THPOTK007



3D edge contribution of the magnet. To minimize the pole height, return-leg winding is used for lowest pole excitation. Also to minimize the longitudinal coil space, one turn longitudinal layer is used. In Fig. 1, a preliminary design of the 3D design is shown. Using 3D FEM analysis (Fig. 2), fields

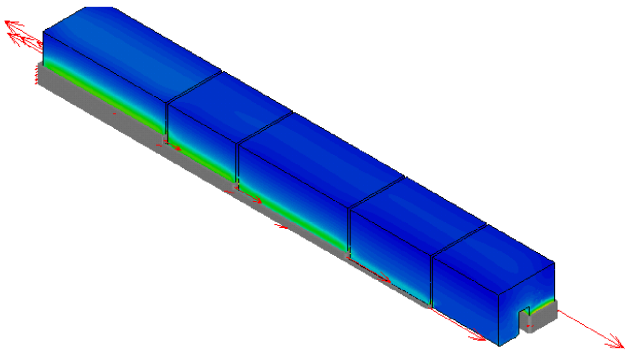

Figure 2: 3D magnetostatic analysis of the LGVM1 magnet.

are calculated. Using the 3D calculated field map with 1 mm 3D mesh, the multipole content along the orbit is calculated and the results is shown in Fig. 3. Figure 3 shows that the multipole components are negligible except the quadrupole component that comes from the edge focusing. Because,

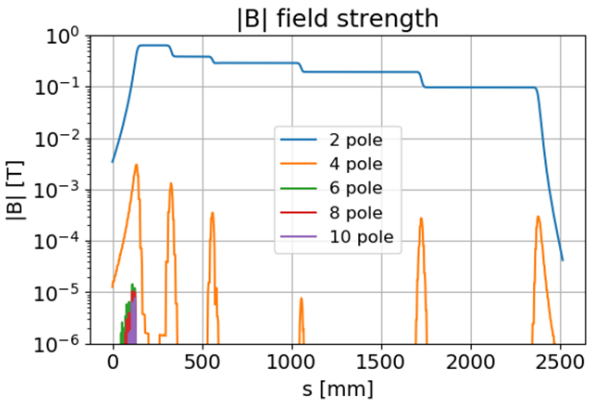


Figure 3: Multipole contents along the trajectory.

the number of turns are quantized, it is impossible to match the design field for all segments. To overcome this issue, small reluctance gap is introduced in the each return leg of the segment to match the design field suggested by the beam dynamics group. Also studies are going on to study the sensitivity of the beam emittance on the field distribution of the segment. If the emittance is not so sensitive, the reluctance gap can be removed while simulating the field profile approximately with matching bending angle and 2nd field integral. The major parameters of the LGBM magnets are shown in the Table 1.

### *Quadrupoles, Quad-bends Magnets*

Three mechanical kinds of Quad-Bends are expected while 3 kinds of mechanical quadrupole types are required. Quadrupole bore radius is 15 mm with different longitudinal

Table 1: Major Parameters of LGBM1, LGBM2 Magnet

| Parameter | LGBM1 | LGBM2 |
|---|---|---|
| Magnet Type | LGBM1A/B | LGBM2A/B |
| Required Num. | 28/28 | 28/28 |
| B range | 0.631T-0.132T | 0.305T-0.153 T |
| Uni. \|x\| < 13 mm | < 1.0E-3 | < 1.0E-3 |
| Min. Pole gap. | 27.8 mm | 24.4 mm |
| Total Length | 2.2348 m | 1.9847 m |
| Trim winding | Yes | Yes |
| Amp. Turns/pole | 7.27 kA | 3.08 kA |
| Conductor | 11.5x11.5x7.5$\phi$ | 9.0x9.0x5.0$\phi$ |
| Num. Turns | 24 | 16 |
| Imax [A] | 303.1 | 192.8 |
| Js [A/mm$^2$] | 3.48 | 3.19 |
| V | 15.8 | 8.70 |
| # Cooling Circuit | 2 | 2 |
| $\Delta$T [K] | 8.3 | 6.5 |
| $\Delta$p | 6.0 bar | 6.0 bar |

magnetic length. Quad-bends have 3 kinds bore radius of 15, 20, 30 mm requirement coming from the vacuum design. Pole shims are introduced in dipole geometry and the geometry is translated to quadrupole geometry using the conformal map given by

$$w = u + iv = \frac{(x + iy)^2}{2R_c} \tag{4}$$

The field quality in quadrupole geometry is calculated while changing the shim geometry in the dipole plane. Figure 4 shows the dipole geometry (left), and quadrupole geometry (right). After 2D optimization, 3D calculations are done to assess the longitudinal dependence of the fundamental and higher harmonic content. Figure 5 shows one example

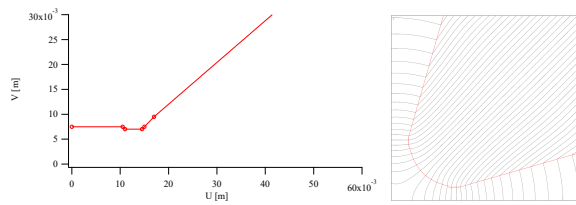


Figure 4: Dipole to qadrupole conformal mapped geometry.

of the quadrupole 3D the results of the calculation showing B distribution. In Fig. 6, the longitudinal distribution of field gradient, and the first two allowed harmonics are shown. Left figure shows the longitudinal dependence of $B'$ estimating the effective length, the right figure shows the longitudinal dependence of two allowed harmonics (B6, B10) at good field radius of 10 mm. The calculated B6 shows a contribution at the edge. The integrated contents are still well within the specification. Major parameter of the quadrupole magnets are shown in Table 2.

ISBN: 978-3-95450-227-1 ISSN: 2673-5490 doi:10.18429/JACoW-IPAC2022-THPOTK007

Table 2: Major Parameters of Quadrupole Magnet

| Parameter | | | |
|---|---|---|---|
| Magnet Type | Q11/Q52 | Q12/31/32 | Q51 |
| Required Num. | 56/56 | 56/56/56 | 56 |
| Max B' [T/m] | 60.0 | 60.0 | 60.0 |
| Multipole | < 1.0E-3 | 1.0E-3 | 1.0E-3 |
| Rc [mm] | 15.0 | 15.0 | 15.0 |
| $L_{eff}$ [m] | 200.0 | 145.0 | 384.0 |
| Trim winding | No | No | No |
| Amp. Turns [kA] | 5.71 | 5.71 | 5.71 |
| Conductor | 6.5x6.5x4$\phi$ | <- | <- |
| Num. Turns | 56 | 56 | 56 |
| Imax [A] | 102.0 | 102.0 | 102.0 |
| Js [A/mm$^2$] | 3.54 | 3.54 | 3.54 |
| V | 9.31 | 7.70 | 14.7 |
| # Cool. Cir. | 2 | 2 | 4 |
| $\Delta$T [K] | 6.5 | 4.9 | 4.7 |
| $\Delta$p [bar] | 6.0 | 6.0 | 6.0 |

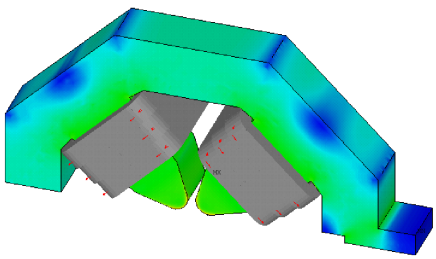

Figure 5: 3D FEM modeling of the quadrupole showing B magnitude distribution.

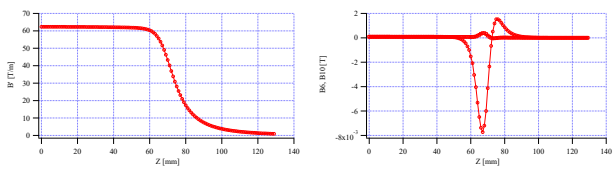

Figure 6: B' distribution (left), B6, B10 at r=10 mm along the magnet(right).

### *Sextupole Magnet*

Only 1 kinds of sextupole design is expected for the storage ring with bore radius of 20 mm, effective length of 250 mm with maximum second derivative B"=2212 T/m$^2$ which gives maximum pole tip field of 0.442 T which is acceptable. The sextupole magent should be laminated since it also should be used as H/V correctors, and skew quadrupole magnet. Minimum pole to pole distance is limited to $\pm$7.0 mm which is coming for slot for synchrotron radiation extraction. It is effectively limiting the pole width deteriorating the field quality. Fortunately, since we are using only 10 mm of aperture, the higher order harmonic could be reduced to a few $10^{-4}$. Like a quadrupole case, pole shims are introduced in dipole geometry and the geometry is translated to sextupole geometry using the conformal map. 2D calculations in sextupole geometry is used to evaluate the effect of the shims. After 2D optimization, 3D calculations are done to assess the longitudinal dependence of the fundamental and higher harmonic content (particularly the fist two allowed harmonic of B9, B15). The results are shown in Fig. 7. The multipole content is order of $3.5 \times 10^{-4}$ which is well within the requirement of $1.0 \times 10^{-3}$.

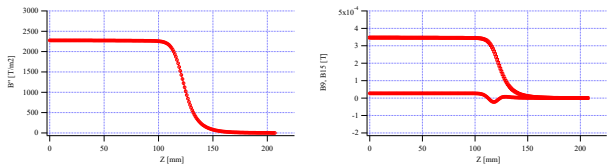

Figure 7: B" distribution (left), B9, B15 at r=10 mm along the magnet(right).

## SUMMARY

Korea 4th generation synchrotron radiation source project has recently started. The design targets 4 GeV, 800 m circumference, 58 pm rad emittances, with 28 periods. The booster at least needs 216 magnet, with additional correctors. Storage ring needs more than 980 magnets. Total magnet system including LTB (Linac to Booser), BTS (Booster to SR), and extraction/extraction magnet reaches 1400 units. In this report, 2D, 3D analysis of the some demanding magnets are carried out with detailed analysis of the longitudinal multipole contents distributions. Detailed engineering designs are also being done to prototype a few important magnets within early 2023.

## ACKNOWLEDGEMENTS

This research was supported in part by the korean Government MSIT (Multipurpose Synchrotron Radiation Construction Project) and by the Basic Science Research Program through the National Research Foundation of Korea (NRF-2019R1A2C1004862).

## REFERENCES

[1] G. S. Jang, S. Shin, M. Yoon, J. Ko, Young Dae Yoon, J. Lee, B-H. Oh, "Low emittance lattice design for Korea-4GSR", *Nuclear Inst. and Methods in Physics Research A*, vol. 1034, p. 166779, 2022. doi:10.1016/j.nima.2022.166779

[2] K. Halbach, "First order perturbation effects in iron-dominated two-dimensional symmetrical multipoles", *Nuclear Instruments and Methods*, vol. 74, pp. 147–164, 1969. doi:10.1016/0029-554X(69)90502-3

[3] M. Borland, T. G. Berenc, R. R. Lindberg, V. Sajaev, and Y. P. Sun, "Lower Emittance Lattice for the Advanced Photon Source Upgrade Using Reverse Bending Magnets", in *Proc. NAPAC'16*, Chicago, IL, USA, Oct. 2016, pp. 877–880. doi:10.18429/JACoW-NAPAC2016-WEPOB01

[4] C. Benabderrahmane *et al.*, "Magnets for the ESRF-EBS Project", in *Proc. IPAC'16*, Busan, Korea, May 2016, pp. 1096–1099. doi:10.18429/JACoW-IPAC2016-TUPMB001